Control of Fusarium wilt disease of tomato and improvement of some growth factors through green synthesized zinc oxide nanoparticles

Aminsajad Jomeyazdian
University of Zabol
Mahdi Pirnia
pirnia@ymail.com

University of Zabol
Hossein Alaei
Rafsanjan University of Vali Asr
Abdolhosein Taheri
Gorgan University of Agricultural Sciences and Natural Resources
Shirahmad Sarani
University of Zabol

Research Article

Keywords: Bio-control, Crop protection, Fungal metabolite, Nanoparticles

Posted Date: August 8th, 2023

DOI: https://doi.org/10.21203/rs.3.rs-3214486/v1

Version of Record: A version of this preprint was published at European Journal of Plant Pathology on February 26th, 2024. See the published version at https://doi.org/10.1007/s10658-024-02831-2.

Abstract

Metabolites from biomass of *Trichoderma harzianum* were used for green synthesis of zinc oxide nanoparticles (ZnONPs) from zinc nitrate ($ZnNO_3$) and GC/MS analysis of metabolite was performed. Then, the antifungal activity of synthesized ZnONPs was evaluated against *Fusarium oxysporum* under the laboratory and greenhouse conditions. Results were compared to different concentrations of Iprodione + Carbendazim (Rovral-TS®) fungicide. Synthesized ZnONPs were characterized by ultraviolet-visible spectrometry (UV-Vis), X-ray diffraction (XRD), transmission electron microscopy (TEM), scanning electron microscopy (SEM) and fourier transform infrared spectroscopy (FTIR). UV-Vis spectra showed an intense peak at 339 nm. X-ray diffraction pattern showed the crystalline nature and purity of the ZnONPs. FTIR revealed various functional groups including phenols, ketones, aldehydes, aliphatic and primary amines, nitriles, alkanes and alkynes in synthesized ZnONPs. Size of ZnONPs determined in the range from 25–60 nm. Based on atomic absorption spectroscopy, foliar application of synthesized ZnONPs, led to considerable accumulation of zinc in the leaves and suitable for compensate zinc deficiency. Some growth factors including root length, root volume, stem length, stem diameter and number of leaves improved in the treatments containing metabolite of *T. harzianum*, $ZnNO_3$ and ZnONPs. Complete inhibition of mycelia growth of *F. oxysporum* was observed in 100 µg/ml concentration of ZnONPs in the laboratory conditions and disease percentage significantly reduced in the greenhouse conditions, indicated that green synthesized ZnONPs gave better results in low concentration than the fungicide. Therefore, application of green synthesized ZnONPs could be recommended as effective alternative and eco-friendly method for crop protection instead chemical fungicides.

Introduction

Tomato (*Solanum lycopersicum* L.) is a globally economic important crop which infected by several fungal diseases. Fusarium wilt caused by *Fusarium oxysporum* Schltdl. is the most destructive soil-borne disease, which limited the cultivation of tomato in the field and greenhouse. Control of soil-borne fungal pathogen by using chemical fungicides carries the risk of soil and groundwater contamination. Some research focused on control of the disease by using chemical fungicide (Amini and Sidovich, 2010) or bio-control agents (El-Sheekh et al. 2022). Compatibility and durability of bio-control agents in the soil has been very controversial. Therefore, using nanoparticles (NPs) have received much attention due to high chemical and thermal stability as well as their antifungal properties (Al-Dhabi and Arasu, 2018).

NPs are nanometer-sized particles that have unique properties and considered as nano-antibiotics due to their antimicrobial activities (Fernando et al. 2018). Antifungal and antibacterial properties of silver NPs (AgNPs) and zinc oxide NPs (ZnONPs) have been further investigated. ZnONPs have antifungal effects against a large number of plant pathogens without toxic effects on plants (Khan et al. 2018) and showed properties such as optical transparency and luminescence properties in the ultraviolet-visible (UV-Vis) range (Ifijen et al. 2022).

Various chemical and physical methods such as sol-gel, hydrothermal, microwave, chemical vapor deposition, ultrasonic and deposition have been developed to prepare ZnONPs. In addition to energy consumption and high cost, these methods contain toxic and dangerous chemicals that lead to biological hazards. In contrast, biological methods (green synthesis) are environmentally friendly in addition to being safe and cost-effective, and used as alternative methods. Furthermore, in green synthesis methods, NPs are produced with better size and properties, compared to physicochemical methods (Akintelu and Folorunso, 2020).

There are limited reports regarding to use metabolites of *Trichoderma* Pers. species for production of NPs. Antifungal and antibacterial properties of silver NPs (AgNPs) and zinc oxide NPs (ZnONPs) have been further investigated. ZnONPs showed effective antifungal effects against *Botrytis cinerea* Pers., *Penicillium expansum* Link and *F. oxysporum* (He et al. 2011; Yehia and Ahmed, 2013). Boruah and Dutta (2021) confirmed that a mixture of *Trichoderma asperellum* Samuels, Lieckf. & Nirenberg and chitosan NPs, suppressed the mycelia growth of *F. oxysporum*, *R. solani* and *Sclerotium rolfsii* Sacc. rather than *Trichoderma* alone and carbendazim 0.1%. Khan et al. (2018) were also reported the effect of ZnONPs in management of some diseases of eggplant.

Antifungal effect of AgNPs mediated by *T. longibrachiatum* Rifai on some phytopathogenic fungi is confirmed (Elamawi et al. 2018). AgNPs mediated by *T. harzianum*, inhibited sclerotia germination and mycelia growth of *Sclerotinia sclerotiorum* (Lib.) de Bary (Guilger et al. 2017). Furthermore, AgNPs synthesized by *T. harzianum*, improved the germination and viability of oil seeds (Shelar and Chaven, 2015). The efficacy of *T. harzianum*-mediated ZnONPs for controlling of three soil-borne pathogens of cotton was evaluated and considerable reduction in seedling disease symptoms is reported (Zaki et al. 2021). *Trichoderma*-mediated ZnONPs were also resulted to synergistic antibacterial effect (Shobha et al. 2020).

The use of fungal metabolites in the biosynthesis of NPs, provides greater stability and can contribute to develop safe nano-fungicides. Therefore, this research carried out in order to green synthesis of ZnONPs and evaluation of their antifungal activity against *F. oxysporum* on tomato. Finally, the results compared with application of different concentrations of Rovral-TS® fungicide.

Materials and Methods

Preparation of fungal isolates

F. oxysporum and *T. harzianum* prepared from fungal culture collection of Vali-e-Asr University of Rafsanjan (Kerman Province, Iran) and transferred to a new PDA culture medium (Merck, Germany).

Production of biomass of T. harzianum

In order to prepare biomass of the fungus, *T. harzianum* grown in liquid culture medium containing 100 ml of GC (0.5% glucose and 0.4% casein hydrolysis) and placed on a rotary shaker with 150 g at 27°C in

an incubator. Biomass separated with sterile whatman filter paper (No. 4), and washed 3 times with sterile deionized water. Then, 20 g of the biomass transferred to an erlenmeyer flask containing 100 ml of sterile distilled water (Elamawi et al. 2018).

Extraction of metabolite

Ethyl acetate was used for extraction of metabolites from fungal biomass. Solvent ethyl acetate was evaporated from the filtrate using a vacuum rotary evaporator at 40°C, 70 rpm and maintained at -20°C. Ethyl acetate extracts were analyzed by Gas Chromatography Mass Spectroscopy (GC/MS).

Green synthesis of ZnNPs

Metabolite of *T. harzianum* mixed with 100 ml of 0.5M solution of zinc nitrate ($(Zn(NO_3)_2$ .4 H_2O, Merck, Germany) and then the mixture placed on a rotary shaker with 100g at 28°C for 72 h. The color change of the culture medium investigated during this period (Rajan et al. 2016).

Characterization of synthesized ZnONPs

UV-Vis Spectroscopy

0.1g of samples were suspended in 100ml distilled water, then placed in an ultrasonic bath (frequency: 37kHz) for 15 min to separate the agglomerated NPs. Resulted suspensions were measured using UNICO spectrophotometer and UV-Vis 4802 model (Ogunyemi et al. 2020).

X-Ray Diffraction (XRD)

The crystallographic characterization was performed utilizing a Philips PW-1730 X-ray diffractometer via a CuKα beam at a wavelength of λ = 1.5418 angstroms. The angle (2θ) ranged from 5 to 40 degrees. to characterize the physicochemical properties of synthesized ZnONPs (Zaki et al. 2021).

Transmission Electron Microscopy (TEM)

TEM analysis was performed to determine the structure and size of the synthesized ZnONPs using Philips EM208S microscope. The samples were placed on a copper grid and the images were analyzed using the Image-J software (Zaki et al. 2021).

Scaning Electron Microscopy (SEM)

Structure, size and agglomeration of synthesized ZnONPs were evaluated with scanning electron microscopy, SEM FEI Quanta 200. Samples coated with a thin layer of Pd/Au and then electron beams are irradiated to them. The images were analyzed using the Image-J software (Shobha et al. 2020).

Fourier Transform Infrared Spectroscopy (FTIR)

FTIR was performed on an AVATAR (Thermo, 370 FTIR, USA) spectrophotometer between wavelengths of 400 cm^{-1} and 4000 cm^{-1}, to reveal organic functional groups or potential bio-molecules involved in the

synthesized ZnONPs and interaction between zinc oxide and biological compounds from fungal metabolites (Nandiyanto et al. 2019).

Atomic absorption spectroscopy

Atomic absorption was performed using Varien SpectrAA 220FS, to determine amount of zinc (Zn) in leaves of tomato, after foliar application of $ZnNO_3$ (0.1mol) and ZnONPs (100µg/ml).

In vitro antifungal activity of synthesized ZnONPs

Synthesized ZnONPs solution placed in an ultrasonic bath (frequency: 37 kHz) for 15 minutes to separate the accumulated nanoparticles. 10, 20, 50 and 100 µg/ml concentration of ZnONPs mixed with PDA culture medium. After coagulation, 5 mm disk of 5-day-old culture of *F. oxysporum* placed in the center of culture medium and incubated at 27°C for 7 days. The growth rate of *F. oxysporum* was investigated during this time. Treatments without NPs with the same conditions were served as controls (Zaki et al. 2021).

In vivo antifungal activity of synthesized ZnONPs

In the greenhouse, the effect of synthesized ZnONPs against *F. oxysporum* was investigated on seedlings of sensitive cultivar of tomato, early-urbana. At first, the soil was autoclaved and tomato seeds were planted in the pots after surface disinfection with sodium hypochlorite (1%) and washing with sterile distilled water. To maintain humidity and prevention from pollution, the pots were covered with plastic lids. Then the spore suspension with concentration of 10^6spores/ml was added to the soil. After 5 days of seedling inoculation, 10ml of synthesized ZnONPs along with fungal metabolites were added to the soil and simultaneously sprayed on the leaves with the same concentration in 3 replications (Zaki et al. 2021). Disease symptoms including yellows and wilting of seedlings were recorded 5 days after last spray.

Antifungal effect of synthesized ZnONPs compared to Rovral-TS® fungicide

Foliar application of ZnONPs suspension with different concentrations was done in 3 repetitions. Iprodione + Carbendazim (Rovral-TS®) fungicide sprayed simultaneously in 3 concentrations (10, 100, 1000 ppm). Disease severity evaluated based on 0–5 scale (0: no symptoms, 1: slight wilting and appearance of brown and necrotic spots in the stem and crown area, 2: disease progress at the level of 30–50%, 3: disease progress at the level of 50–70%, 4: disease progress at the level of 70–90%, 5: complete loss) described by Chikh Rouhou et al. (2010). Disease severity calculated through below formula (n: number of seedlings in each scale).

$$x = \frac{\mathrm{n0} + 1 \times \mathrm{n1} + 2 \times \mathrm{n2} + 3 \times \mathrm{n3} + 4 \times \mathrm{n4} + 5 \times \mathrm{n5}}{5 \times (\mathrm{n0} + \mathrm{n1} + \mathrm{n2} + \mathrm{n3} + \mathrm{n4} + \mathrm{n5})} \times 100$$

Effect of synthesized ZnONPs on some growth factors of tomato

Tomato seeds were sterilized by 70% ethanol (2 min) and 1% sodium hypochlorite (5 min) and washed with distilled water, then planted in a mixture of coco peat and perlite in pots. After seed germination, tomato seedlings were grown in three treatments including 1- Hoagland solution, complete for tomato seedlings, 2- Hoagland solution without zinc element and 3- distilled water. All plants were kept in greenhouse conditions with 150 ml of irrigation solution every week for 4 weeks. Then, treatments containing synthesized ZnONPs were applied to the grown plants. Different levels of NPs (0, 5 and 10 µM) were considered for each treatment. The test was conducted in a completely randomized design in the form of factorial experiments with 3 replications (Sing et al. 2019).

Results

Compounds of metabolite by GC/MS analysis

For determination of compounds in fungal metabolite, the ethyl acetate extract of *T. harzianum* were analyzed by GC/MS and different compounds are recognized (Table 1).

Table 1
Compounds found in metabolite of *T. harzianum* detected by GC/MS analysis. RT: Retention Time

Name of the compound	RT (min)	Percentage
Isobutyl (2-(2-(2-methoxyethoxy) ethoxy) ethyl) carbonate	4.787	0.08
L-Lactic acid	6.086	11.69
1,2-Cyclopentanedione	6.454	1.52
Methoxyacetic acid, 2-pentyl ester	7.095	0.42
3-Ethoxy-1,2-propanediol	8.196	0.57
1,3-Butanediol	9.123	0.26
Butanedioic acid, monomethyl ester	10.539	0.62
Benzenamine, N-ethyl	11.210	0.08
Cyclopropane, 1,2-dimethyl-, cis	11.973	0.22
N-Aminopyrrolidine	13.256	0.68
dl-Mevalonic acid lactone	14.310	0.28
Cyclohexasiloxane, dodecamethyl	15.779	0.08
Benzeneethanol, 4-hydroxy	17.953	0.33
1,3-Cyclopentanedione, 2-ethyl-4-propyl	19.201	0.18
Butylated Hydroxytoluene	19.813	0.36
Benzoic acid, 2-ethylhexyl ester	24.814	0.11
Benzyl Benzoate	26.271	0.53
Isopropyl myristate	27.763	0.30
Hexadecanoic acid, methyl ester	30.275	0.09
Benzenepropanoic acid, 3,5-bis dimethylethyl)-4-hydroxy-, methyl	30.730	0.09
1,2-Benzenedicarboxylic acid, buty l 2-ethylhexyl ester	31.184	0.36
Hexadecanoic acid, ethyl ester	31.954	0.15
2-methyloctacosane	32.076	0.23
Isopropyl palmitate	32.781	0.18
Oleic Acid	36.593	0.14
Tetrahydroionyl acetate	37.602	0.09

Name of the compound	RT (min)	Percentage
Cyclooctene, 3-(1-methylethenyl)	38.575	0.11
Octadecane, 3-ethyl-5-(2-ethylbutyl)	41.472	0.11
Phthalic acid, 6-ethyloct-3-yl 2-ethylhexyl ester	43.331	0.36
Phthalic acid, furfuryl propyl ester	43.413	0.30
Bis(2-ethylhexyl) phthalate	44.223	69.19
Terephthalic acid, 2-ethylhexyl oc tyl ester	47.242	1.25

UV-Vis Spectroscopy

UV-Vis spectra of *T. harzianum*-mediated ZnONPs and $ZnNO_3$ solution, represented an intense peak at 339 nm in synthesized ZnONPs (Fig. 1).

XRD analysis

X-ray diffraction test is used for evaluating the properties of crystals. The XRD pattern revealed the crystal structure of the synthesized ZnONPs. In the diffraction pattern of synthesized ZnONPs, one broad peak at an angle of about 36° was observed, indicated the octahedral and crystalline nature as well as creation of an amorphous structure in synthesized ZnONPs (Fig. 2). The distance between the crystal planes were increased, when organic compounds in the metabolite placed on the crystal structure of $ZnNO_3$.

Transmission electron microscope (TEM)

TEM images showed octahedral shapes with a crystalline structure of ZnONPs, with dimensions between 25–50 nm (Fig. 3). NPs were observed as complexes in separate clusters. The octahedral pattern observed in this method was the same as the pattern analyzed by XRD.

Scaning Electron Microscopy (SEM)

SEM analysis of synthesized ZnONPs showed spherical and octahedral shapes of nanoparticles in aggregated state (Fig. 4). Size of synthesized ZnONPs determined in the range of 30–60 nm. Analysis of SEM images confirmed the size distribution observed by TEM.

Fourier transform infrared spectroscopy (FTIR)

In the FTIR spectrum, the peak of the stretching vibration of O-H bonds in the hydroxyl groups occurred at wavelengths of 3300 cm^{-1} to 3600 cm^{-1}. The bending vibration of this bond and the stretching vibration of C = C bonds in aromatic rings were placed at a wavelength of 1630 cm^{-1} (Nandiyanto et al. 2019). The peaks located at 2960 cm^{-1} and 2870 cm^{-1} related to the asymmetric and symmetric stretching vibrations of C-H bonds in the methyl and methylene structures of the components, respectively (Jung et al. 2018). The peak located at 1740 cm^{-1} related to the stretching vibration of C = O bonds in carbonyl

and carboxyl structures. Peaks at 1450 cm^{-1} and 1370 cm^{-1} related to the bending vibration of bonds C-H in methyl and methylene structures, respectively (Shahmoradi et al. 2021). In addition, peaks at 1240 cm^{-1} and 1040 cm^{-1} related to the stretching vibrations of C-OH and C-O-C bonds in the chemical components (Feng et al. 2014; Jung et al. 2018). Also, the bending vibration of C-H bonds on cyclo structures caused an absorption peak at 494 cm^{-1} (Feng et al. 2014). The peak at about 1635 cm^{-1} became sharper, possibly because hydrogen bonds occurred between the compounds in fungal metabolite and $ZnNO_3$. Another reason could be the presence of aromatic components in fungal metabolite. An increase in the intensity of the peaks related to fungal metabolite and an increase in the prevalence of hydrogen bonds between $ZnNO_3$ and components of metabolite were observed.

Atomic absorption spectroscopy

After foliar spray of treatments containing zinc (Zn), atomic absorption spectroscopy revealed significant difference in absorption of zinc (Zn) among treatments. Maximum absorption was belonged to $ZnNO_3$ (132 ppm). Absorption through ZnONPs was recorded between 78–88 ppm (Fig. 6).

In vitro antifungal activity of synthesized ZnONPs

The control potential of synthesized ZnONPs to inhibit the radial growth of *F. oxysporum* was investigated by growing fungus in plates containing 10, 20, 50 and 100 µg/ml concentration of ZnONPs. As shown in the figure (7), the radial growth rate and development of *F. oxysporum* decreased in all treatments containing ZnONPs. High levels of concentrations, showed the maximum inhibition of radial growth.

In vivo assessment of different treatments on disease symptoms and disease development

In greenhouse conditions, different treatments were evaluated for their ability to reduce Fusarium wilt disease. Disease symptoms and development decreased significantly in treatments containing $ZnNO_3$ and ZnONPs + metabolite (Figs. 8, 9).

Disease percentage in different treatments compared to fungicide

Disease percentage in seedlings treatment with ZnONPs + metabolite of *T. hazianum* + *F. oxysporum* (average: 17%) was nearly equal with application of 1000 ppm concentration of Iprodione + Carbendazim fungicide. In other treatments, high levels of disease were observed (Fig. 10).

Effect of different treatment on some growth factors of tomato

In a greenhouse, different treatments were tested for their ability to improve tomato growth factors and reduce Fusarium wilt disease. In root volume, the highest level belonged to ZnONPs + metabolite (Fig. 11). $ZnNO_3$ showed maximum level in root length (Fig. 12). In treatments containing $ZnNO_3$ and ZnONPs + metabolite, stem length were more than others (Fig. 13). Stem diameter in $ZnNO_3$ and ZnONPs + metabolite treatments showed the same average (Fig. 14). Number of leaves in treatments containing ZnONPs, were higher than others, whereas treatments inoculated with *F. oxysporum* showed lower levels (Fig. 15).

Discussion

Metabolites of *T. harzianum* contained a variety of compounds that can play an important role in biosynthesis of ZnONPs. GC/MS analysis revealed that metabolite of *T. harzianum* is an appropriate source of compounds which are contributed in biosynthesis of ZnONPs. The results were nearly close to the previous research (Siddiquee et al. 2012; Shobha et al. 2020).

100 µg/ml of synthesized ZnONPs, completely prevented the radial growth of *F. oxysporum*, which was nearly equal to application of 1000 ppm concentration of Rovral-TS® fungicide in greenhouse conditions. Application of ZnONPs and $ZnNO_3$ were also caused improvement in some growth factors, which in agreement with the results of previous researches (Shobha et al. 2020; Zaki et al. 2021). Atomic absorption analysis showed that foliar spray of ZnONPs and $ZnNO_3$ provided high level accumulation of zinc in leaves and improved zinc deficiency in tomato. The results were in agreement with Jitao et al. (2015) and Khan et al. (2015), who reported that foliar application of ZnONPs was more effective than seed priming.

The UV-Vis spectrum of synthesized ZnONPs showed absorption band at 339 nm, nearly similar to the results of Zaki et al. (2021), who reported maximum absorption at 300 nm. Perveen et al. (2020) reported the peak at 300 nm in ZnONPs synthesized by Sol-Gel method. The UV-Vis spectrum of ZnONPs synthesized by *Aspergillus niger* Tiegh., showed absorption band at 390 nm (Gao et al. 2019), which nearly in agreement with our results of present study.

TEM imaging confirmed the synthesis of ZnONPs with dimensions between 25 and 50 nm. Due to higher resolution and larger depth of field, SEM images revealed more details of the surface of various NPs (Elumalai et al. 2015). However, TEM images have a higher resolution in measuring NPs than SEM (Nain et al. 2020). XRD analysis confirmed the octahedral structure and crystalline nature of ZnONPs. Unlike chemical methods, in the green synthesis of NPs, the impurities were not observed. FTIR analysis showed that the synthesized ZnONPs were well placed among the metabolite structure of *T. harzianum* and strong bonds were formed between their molecules. Various functional groups including phenols, ketones, aldehydes, aliphatic and primary amines, nitriles, alkanes and alkynes were recognized by FTIR spectra. Peak observed at 1635 cm^{-1} corresponded to N–H bend of fungal biomass, in agreement with the results of Zaki et al. (2021), which peak at 1629 cm^{-1}, was attributed to the fungal biomass.

Based on high level of impact on fungal pathogen as well as less cost and bio-environmental advantages over fungicides, green production of ZnONPs gave better results against *F. oxysporum* and help to provide higher quality products.

Conclusion

T. harzianum-mediated ZnONPs can recommend as safe and eco-friendly method for controling Fusarium wilt disease, improvement of zinc deficiency in tomato and reduction of utilization fungicides.

Declarations

Acknowledgment

This work was funded by University of Zabol, Grant number: IR-UOZ-GR-7062. The authors would like to thank the Research Deputy of University of Zabol for financial support.

Compliance with Ethical Standards

-Disclosure of potential conflicts of interest:

The authors declare no conflict of interest.

-Research involving Human Participants and/or Animals

This research focused on green synthesis of ZnONPs and their antifungal effect on Fusarium wilt disease of tomato.

-Informed consent

The authors are satisfied to publish this work in European Journal of Plant Pathology.

References

1. Akintelu, S.A, & Folorunso, A.S. (2020). A review on green synthesis of zinc oxide nanoparticles using plant extracts and its biomedical applications. *BioNanoScience, 10*(4), 848–863.
2. Al-Dhabi, N.A., & Valan Arasu, M. (2018). Environmentally-friendly green approach for the production of zinc oxide nanoparticles and their anti-fungal, ovicidal, and larvicidal properties. *Nanomaterials, 8*(7), 500.
3. Amini, j., & Sidovich, D.F. (2010). The effects of fungicides on *Fusarium oxysporum* f. sp. *lycopersici* associated with Fusarium wilt of tomato. *Journal of Plant Protection Research, 50*(2), 172–178.
4. Boruah, S., & Dutta, P. (2021). Fungus mediated biogenic synthesis and characterization of chitosan nanoparticles and its combine effect with *Trichoderma asperellum* against *Fusarium oxysporum*, *Sclerotium rolfsii* and *Rhizoctonia solani*. *Indian Phytopathology, 74*, 81–93.

5. Chikh-Rouhou, H., González-Torres, R., & Alvarez, J.M. (2010). Screening and morphological characterization of melons for resistance to *Fusarium oxysporum* f.sp. *melonis* Race 1.2. *Horticultural Sciences, 45*(7), 1021–1025.
6. Elamawi, R.M., Al-Harbi, R.E., & Hendi, A.A. (2018). Biosynthesis and characterization of Silver nanoparticles using *Trichoderma longibrachiatum* and their effect on phytopathogenic Fungi. *Egypt J. Biol. Pest Control, 28*, 28.
7. El-Sheekh, M.M., Deyab, M.A., Hasan, R.S.A., Abu Ahmed, S.E., & Elsadany, A.Y. (2022). Biological control of Fusarium tomato-wilt disease by cyanobacteria *Nostoc* spp. *Archives of Microbiology, 204*(1),116. doi: 10.1007/s00203-021-02673-0.
8. Elumalai, K., Velmurugan, S., Ravi, S., Kathiravan, V., & Adaikala Raj, G. (2015). Bio-Approach: Plant Mediated Synthesis of ZnO Nanoparticles and Their Catalytic Reduction of Methylene Blue and Antimicrobial Activity. *Adv. Powder Technol, 26*, 1639–1651.
9. Feng, Y., Feng, N., Wei, Y., & Zhang, G. (2014). An *in situ* gelatin-assisted hydrothermal synthesis of ZnO–reduced graphene oxide composites with enhanced photocatalytic performance under ultraviolet and visible light. *RSC Advances, 4*, 7933.
10. Fernando, S., Gunasekara, T., & Holton, J. (2018). Antimicrobial nanoparticles: applications and mechanisms of action. *Sri Lankan Journal of Infectious Diseases,* https://doi.org/10.4038/sljid.v8i1.8167.
11. Gao, Y., Anand, M., Ramachandran, V., Karthikkumar, V., Shalini, V., Vijayalakshmi, S., & Ernest, D. (2019). Biofabrication of Zinc Oxide Nanoparticles from *Aspergillus niger*, Their Antioxidant, Antimicrobial and Anticancer Activity. *J. Clust. Sci, 30*, 937–946.
12. Guilger, M., Pasquoto-Stigliani, T., Bilesky-Jose, N., Grillo, R., Abhilash, P.C., Fraceto, L.F., & De Lima, R. (2017). Biogenic silver nanoparticles based on *Trichoderma harzianum*: Synthesis, characterization, toxicity evaluation and biological activity. *Sci. Rep, 7*, 44421.
13. He, L., Liu, Y., Mustapha, A., & Lin, M. (2011). Antifungal Activity of Zinc Oxide Nanoparticles against *Botrytis Cinerea* and *Penicillium expansum*. *Microbiol. Res, 166*, 207–215.
14. Ifijen, I.H., Maliki, M., & Anegbe, B. (2022). Synthesis, photocatalytic degradation and antibacterial properties of Selenium or Silver doped Zinc oxide nanoparticles: A detailed review. *OpenNano,* 100082.
15. Jitao, L. V., Zhang, S., Luo, L., Zhang, J., Yang, K., & Christied, P. (2015). Accumulation, speciation and uptake pathway of ZnO nanoparticles in maize. *Environ. Sci. Nano, 2*, 68.
16. Jung, M.R., Horgen, F.D., Orski, S.V., Rodriguez, V., Beers, K.L., Balazs, G.H., Jones, T.T., Work, T.M., Brignac, K.C., Royer, S.J., Hyrenbach, K.D., Jensen, B.A., & Lynch, J.M. (2018). Validation of ATR FT-IR to identify polymers of plastic marine debris, including those ingested by marine organisms. *Marine Pollution Bulletin, 127*, 704–716.
17. Khan, M., & Siddiqui, Z.A. (2018). Zinc oxide nanoparticles for the management of *Ralstonia solanacearum, Phomopsis vexans* and *Meloidogyne incognita* incited disease complex of eggplant. *Indian Phytopathology, 71*(3), 355–364.

18. Nain, V., Kaur, M., Sandhu, K.S., Thory, R., & Sinhmar, A. (2020). Development, Characterization and Biocompatibility of Zinc Oxide Coupled Starch Nanocomposites from Different Botanical Sources. *Int. J. Biol. Macromol, 162*, 24–30.
19. Nandiyanto, A.B.D., Oktiani, R., & Ragadhita, R. (2019). How to Read and Interpret FTIR Spectroscope of Organic Material. *Indonesian Journal of Science and Technology, 4*, 97.
20. Ogunyemi, S.O., Abdallah, Y., Zhang, M., Fouad, H., Hong, X., Ibrahim, E., & Li, B. (2019). Green synthesis of zinc oxide nanoparticles using dierent plant extracts and their antibacterial activity against *Xanthomonas oryzae* pv. *oryzae*. *Artif. Cells Nanomed. Biotechnol, 47*, 341–352.
21. Perveen, R., Shujaat, S., Qureshi, Z., Nawaz, S., Khan, M.I., & Iqbal, M. (2020). Green versus Sol-Gel Synthesis of ZnO Nanoparticles and antimicrobial activity evaluation against panel of pathogens. *J. Mater. Res. Technol, 9*, 7817–7827.
22. Rajan, A., Cherian, E., &Baskar, G. (2016). Biosynthesis of zinc oxide nanoparticles using *Aspergillus fumigatus* JCF and its antibacterial activity. I*nt. J. Mod. Sci. Technol, 1*, 52–57.
23. Shahmoradi, A.R., Talebibahmanbigloo, N., Nickhil, C., Nisha, R., Javidparvar, A.A., Ghahremani, P., Bahlakeh, G., & Ramezanzadeh, B. (2021). Molecular-MD/atomic-DFT theoretical and experimental studies on the *quince seed* extract corrosion inhibition performance on the acidic-solution attack of mild-steel. *Journal of Molecular Liquids,* 117921.
24. Shelar, G.B., & Chavan, A.M. (2015). Myco-synthesis of silver nanoparticles from *Trichoderma harzianum* and its impact on germination status of oil seed. *Biolife, 3*, 109–113.
25. Shobha, B., Lakshmeesha, T.R., Ansari, M.A., Almatroudi, A., Alzohairy, M.A., Basavaraju, S., Alurappa, R., Niranjana, S.R., & Chowdappa, S. (2020). Mycosynthesis of ZnO nanoparticles using *Trichoderma* spp. isolated from rhizosphere soils and its synergistic antibacterial Effect against *Xanthomonas oryzae* pv. *oryzae. J. Fungi, 6*, 181.
26. Siddiquee, S., Cheong, B.E., Taslima, K., Kausar, H., & Hasan, M.M. (2012). Separation and identification of volatile compounds from liquid cultures of *Trichoderma harzianum* by GC-MS using three dierent capillary columns. *J. Chromatogr. Sci, 50*, 358–367.
27. Singh, J., Kumar, S., Alok, A., Upadhyay, S.K., Rawat, M., Tsang, D.C., Bolan, N., & Kim, K.H. (2019). The potential of green synthesized zinc oxide nanoparticles as nutrient source for plant growth. *Journal of Cleaner Production, 214*, 1061–1070.
28. Yehia, R.S., & Ahmed, O.F. (2013). In Vitro Study of the Antifungal Efficacy of Zinc Oxide Nanoparticles against *Fusarium oxysporum* and *Penicilium expansum*. *Afr. J. Microbiol. Res, 7*, 1917–1923.
29. Zaki, S.A., Ouf, S.A., Albarakaty, F.M., Habeb, M.M., Aly, A.A., & Abd-Elsalam, K.A. (2021). *Trichoderma harzianum*-mediated ZnO nanoparticles: A green tool for controlling soil-borne pathogens in Cotton. *J. Fungi, 7*, 952. https://doi.org/10.3390/jof7110952.

Figures

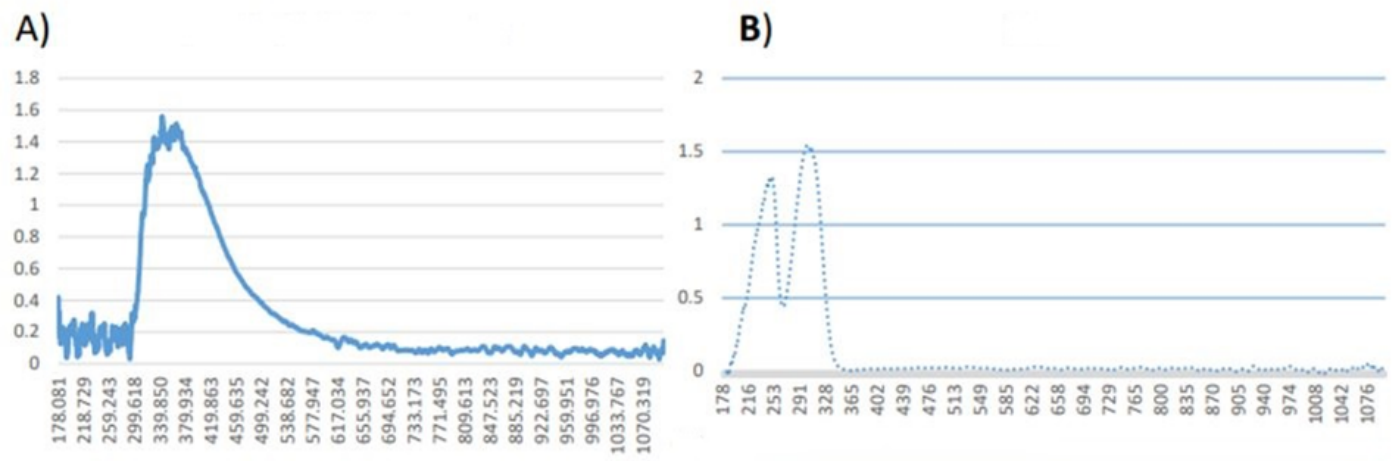

Figure 1

UV-Vis spectra of *T. harzianum*-mediated ZnONPs (A) and $ZnNO_3$ solution (B)

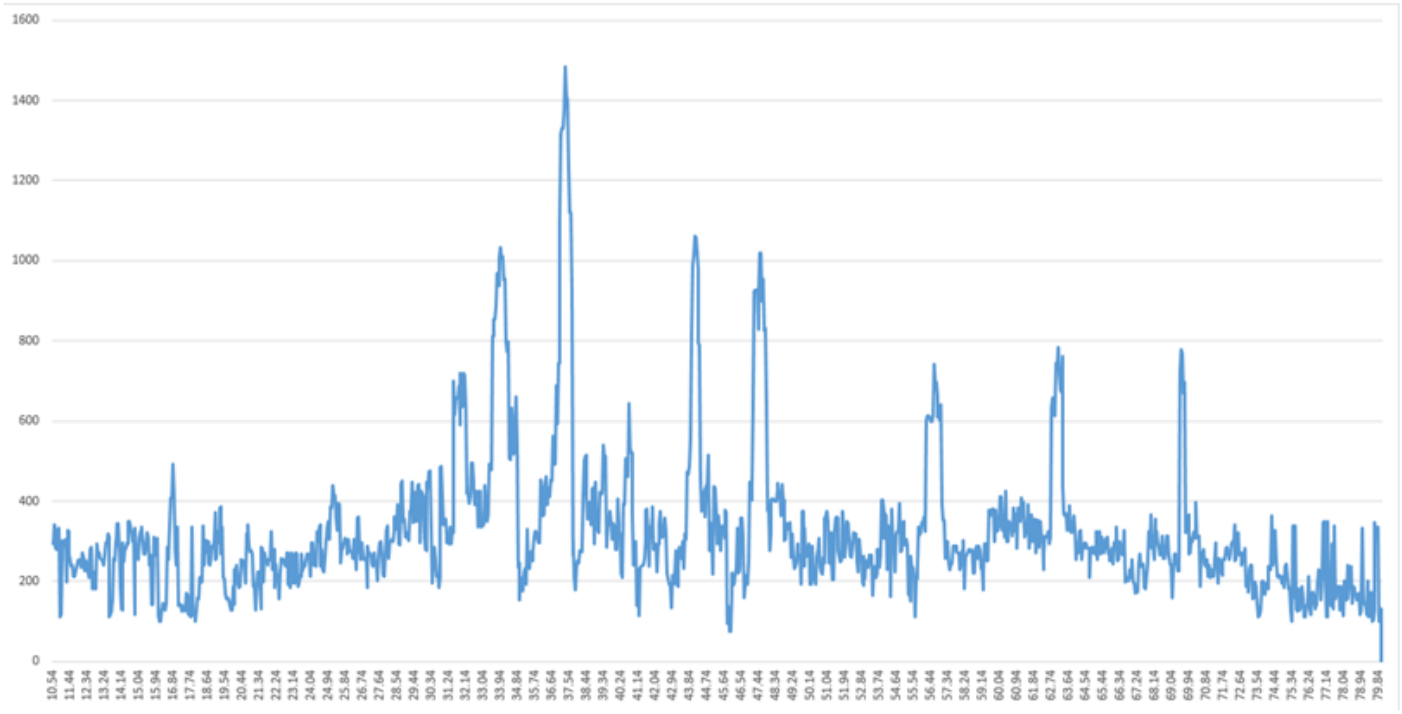

Figure 2

X-ray diffraction pattern of *T. harzianum*-mediated ZnONPs.

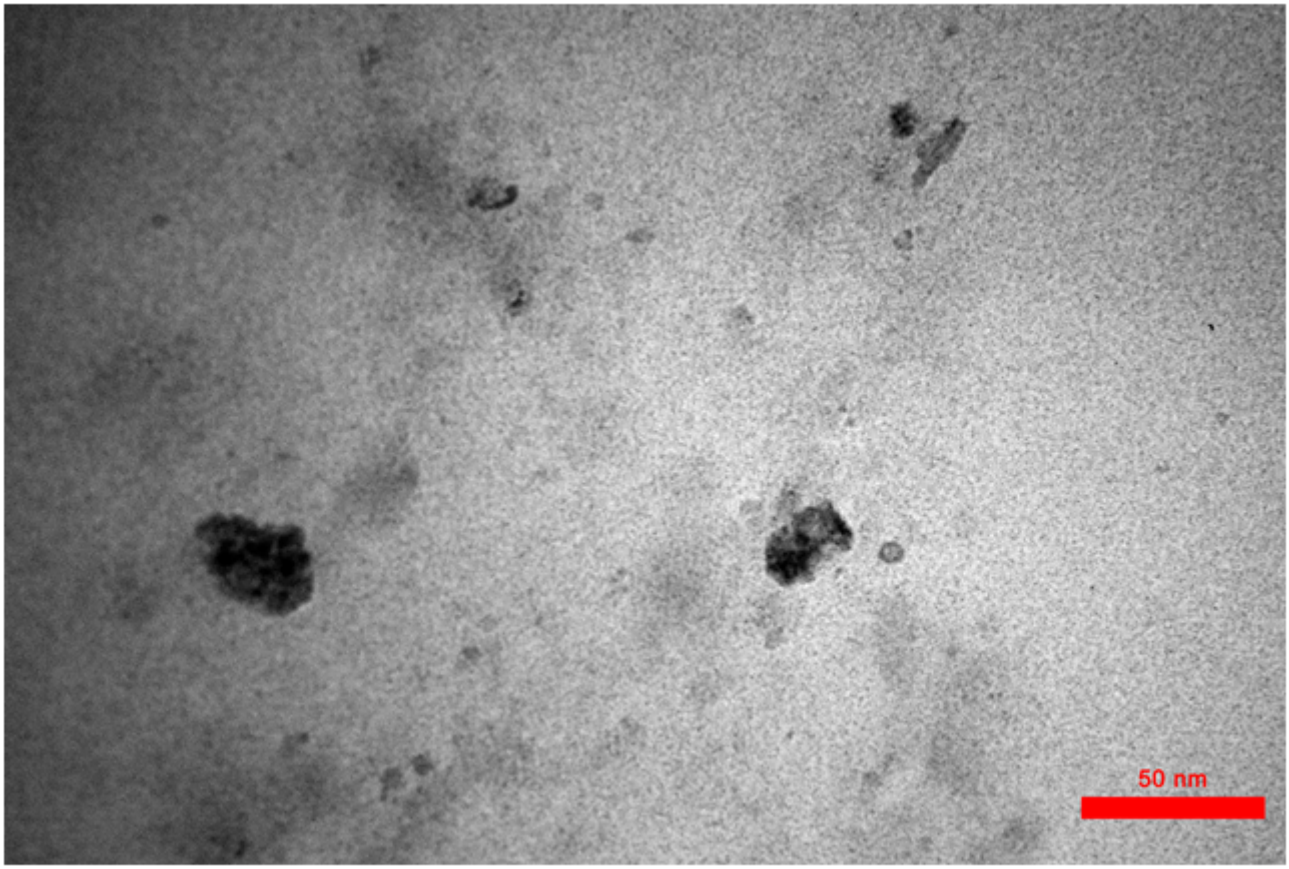

Figure 3

TEM image of *T. harzianum*-mediated ZnONPs

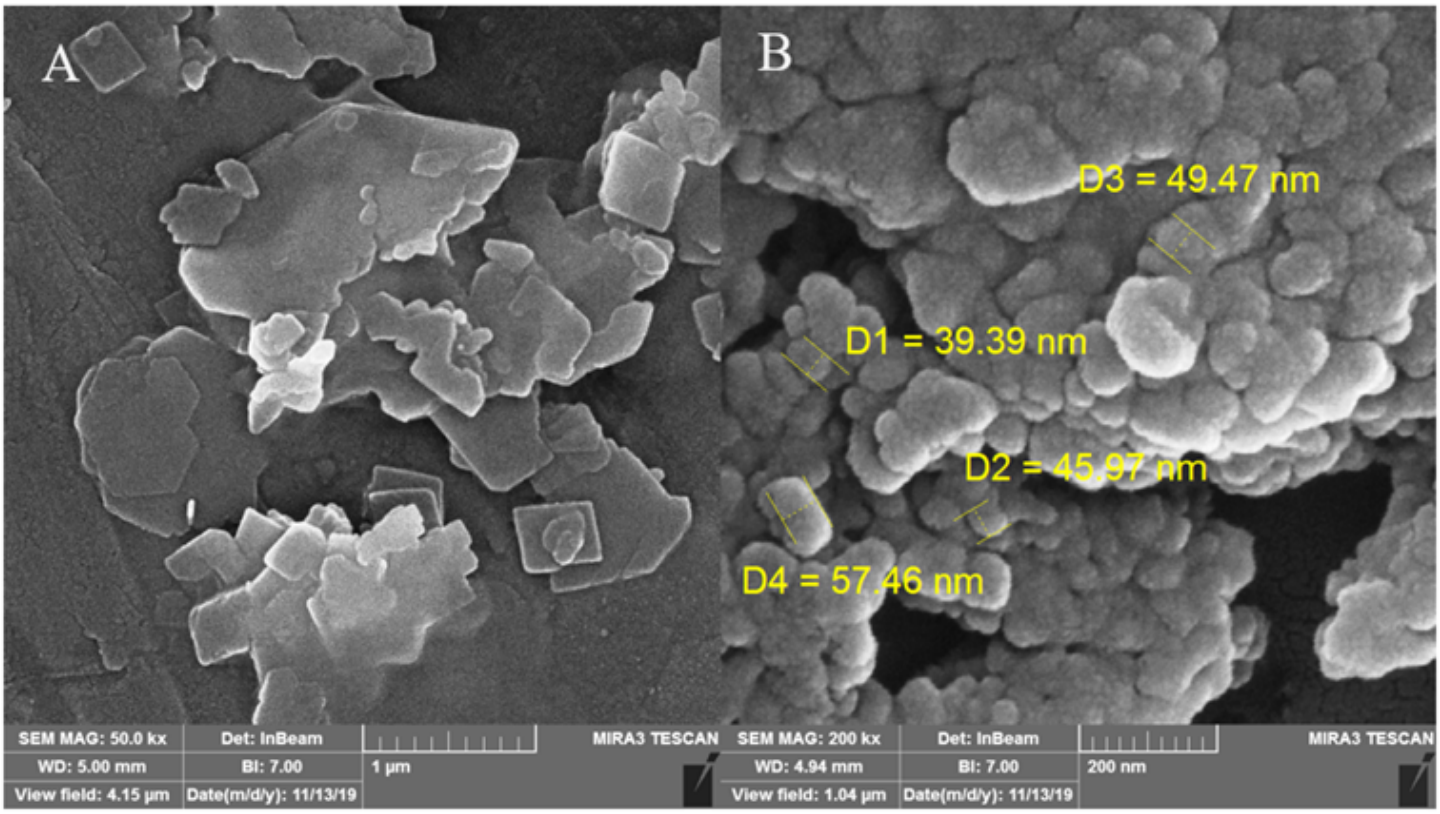

Figure 4

SEM micrographs (A): Zinc Nitrate ($ZnNO_3$), (B): ZnONPs mediated by *T. harzianum*.

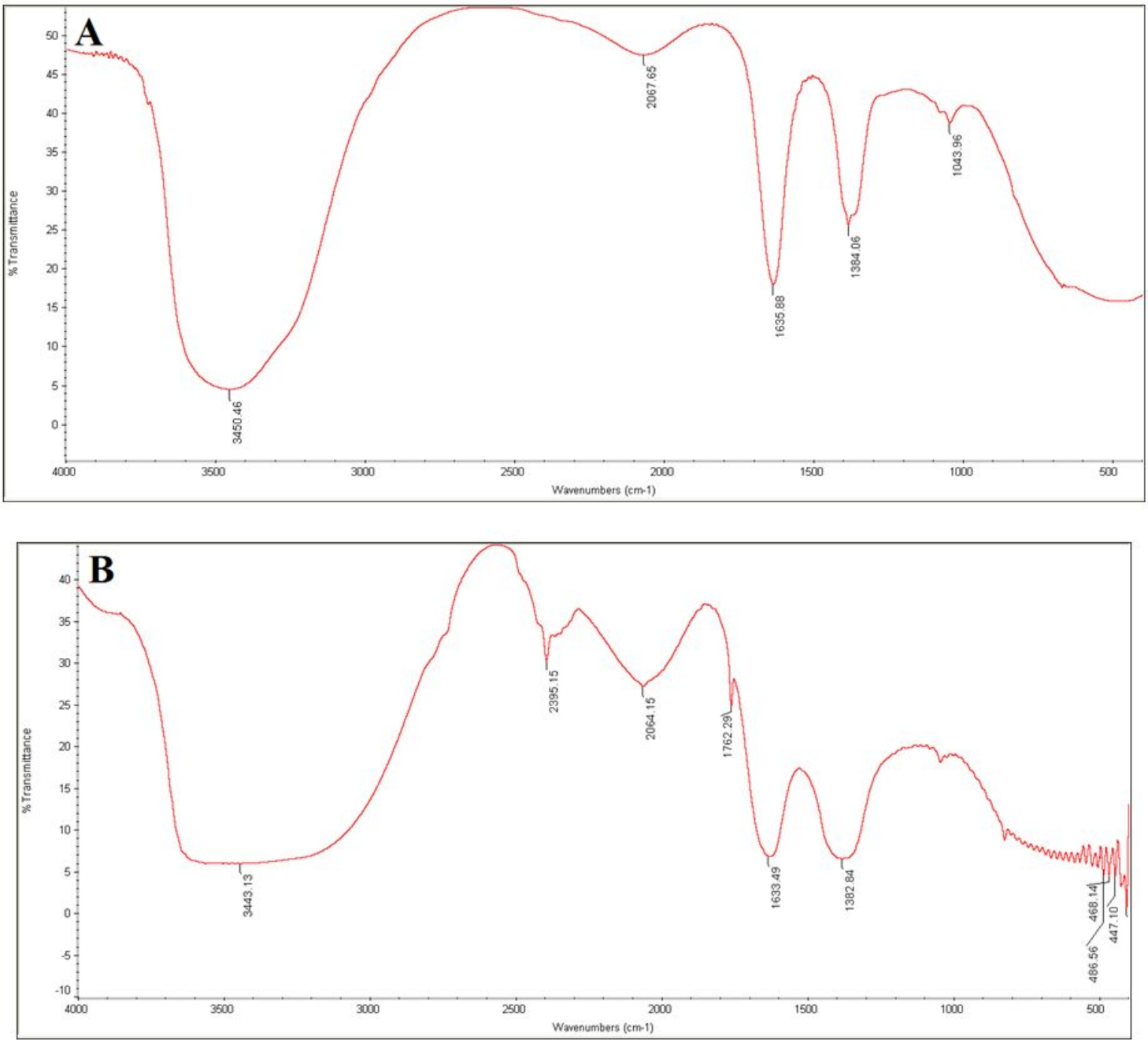

Figure 5

FTIR Spectrum of (A): *T. harzianum*-mediated ZnONPs and (B): $ZnNO_3$ solution

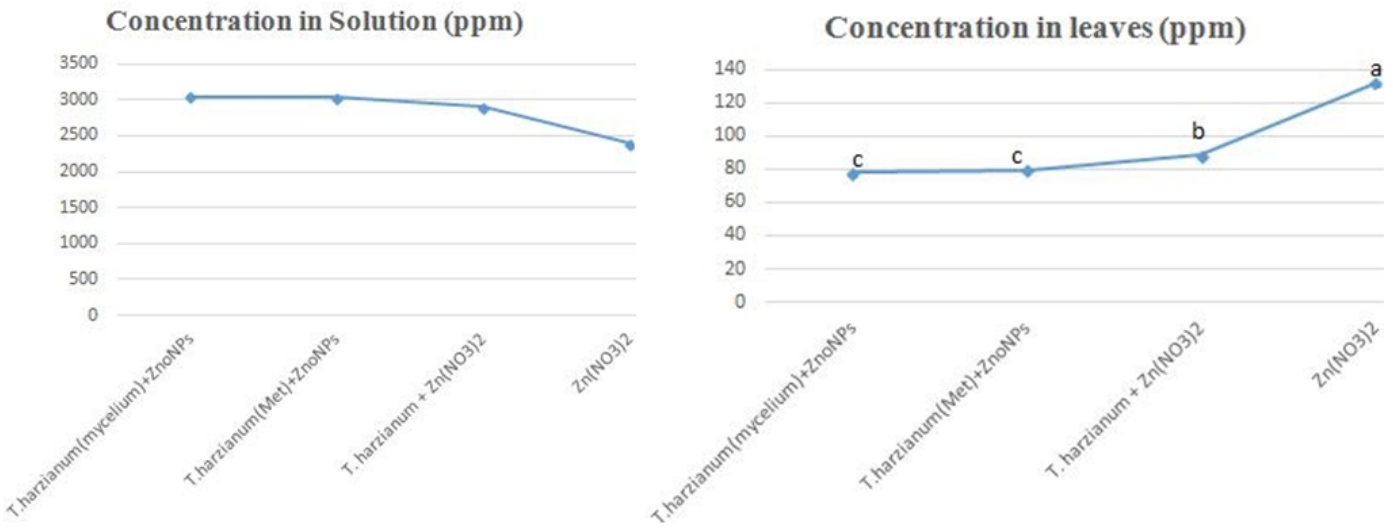

Figure 6

Left: Concentration of Zinc (Zn) in initial solution; Right: Absorption of Zinc in leaves after treatments

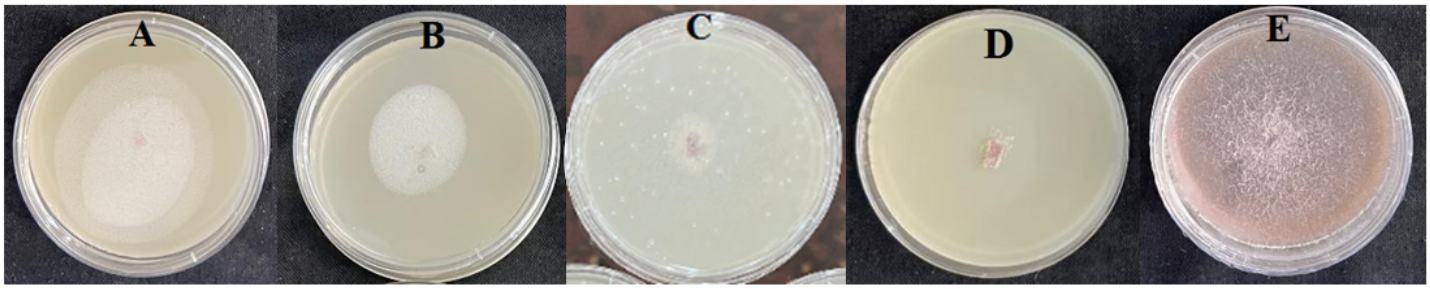

Figure 7

Inhibition of radial growth of *F. oxysporum* on PDA containing ZnONPs at different concentrations: (A) 10 µg/ml, (B) 20 µg/ml, (C) 50 µg/ml, (D) 100 µg/ml, (E) Control after 7 days.

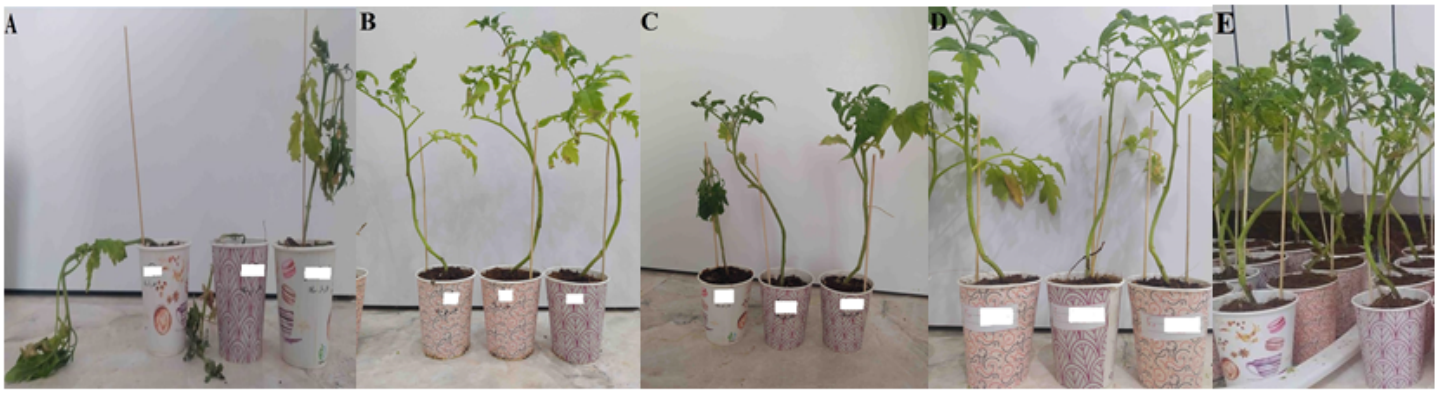

Figure 8

Symptoms in different treatments of experiment (A): wilting symptoms on seedlings inoculated by *F. oxysporum* (B): *F. oxysporum*+metabolite of *T. harzianum* (C): *F. oxysporum*+$ZnNO_3$ (D): *F. oxysporum*+ZnONPs+metabolite of *T. harzianum* (E): Control

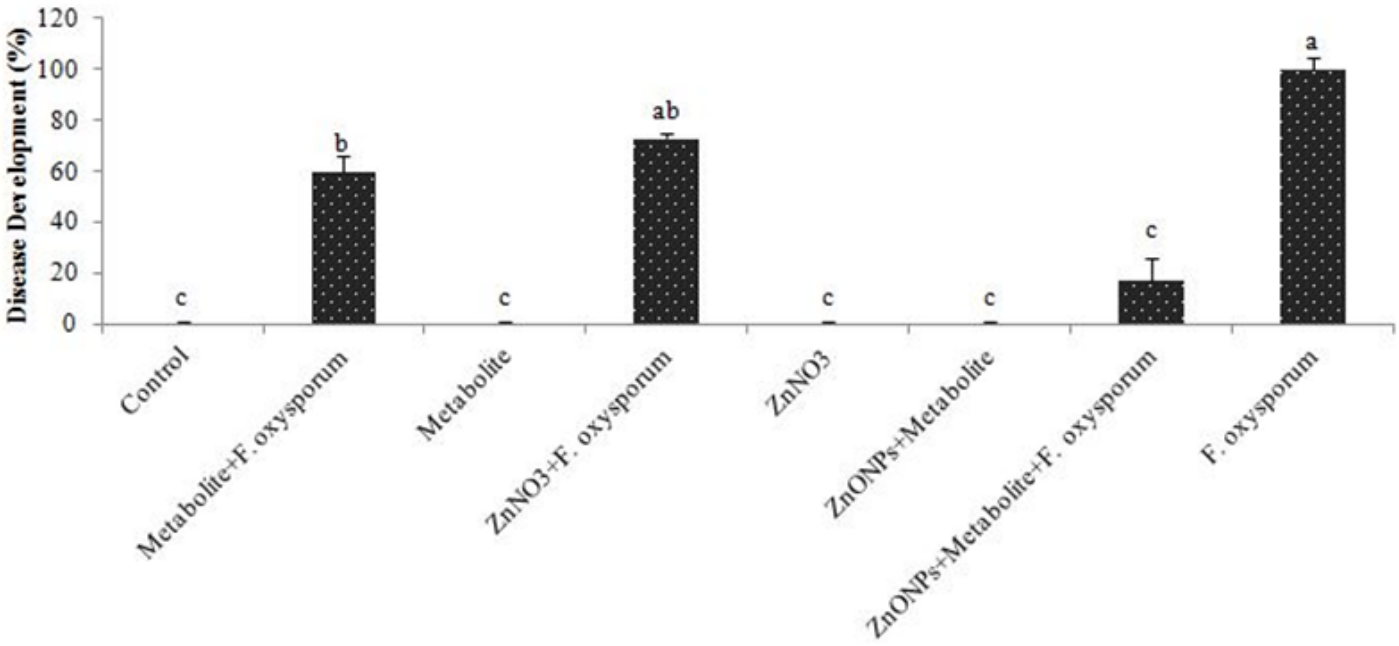

Figure 9

Disease development in different treatments

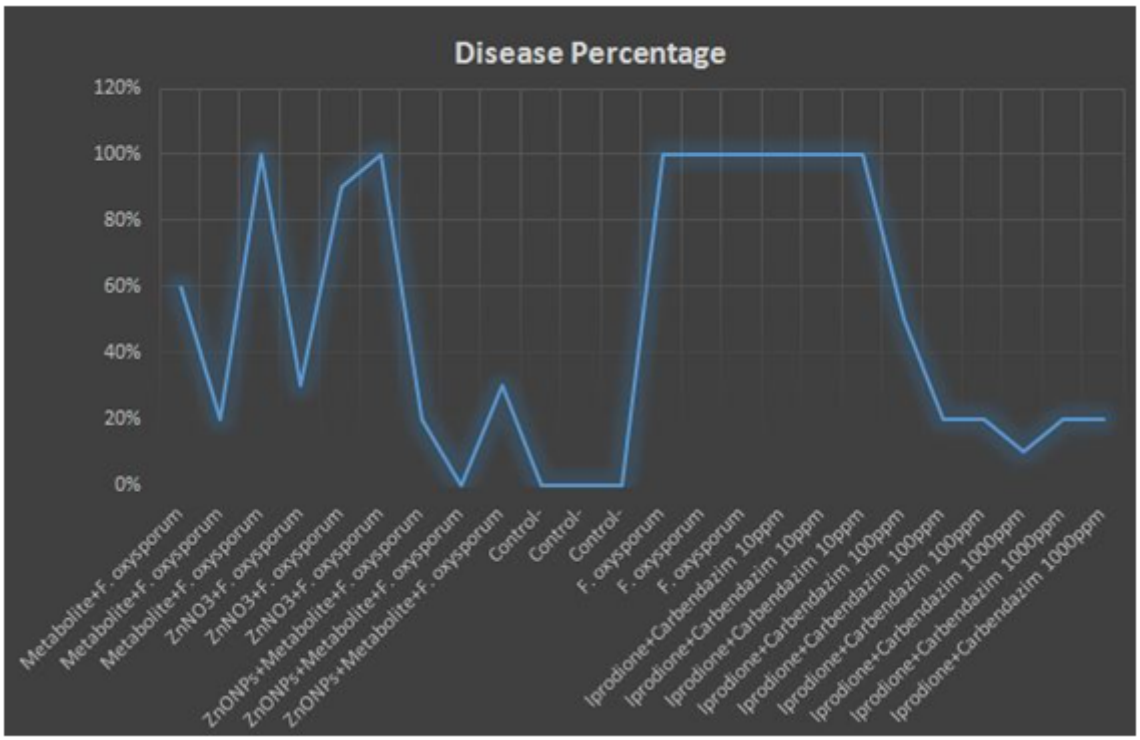

Figure 10

Disease percentage in different treatments with 3 repetitions compared to different concentrations of Iprodione+Carbendazim fungicide

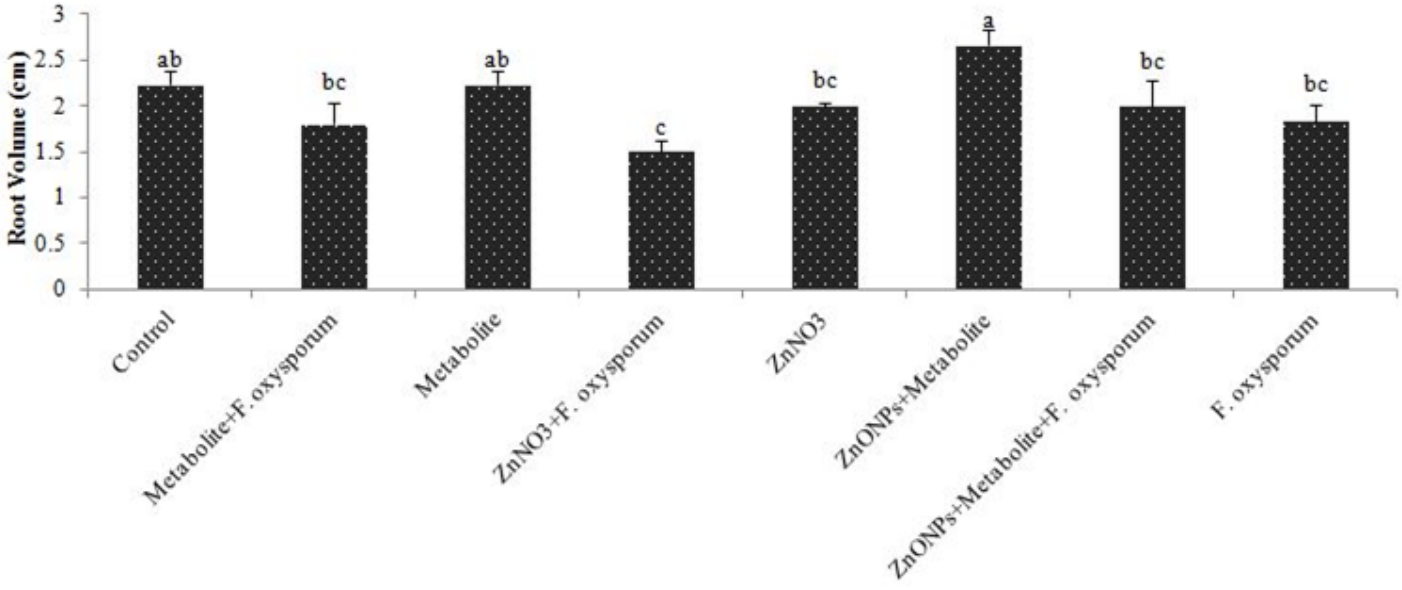

Figure 11

Improve of root volume in treatments containing metabolite of *T. harzianum*, $ZnNO_3$ and ZnONPs.

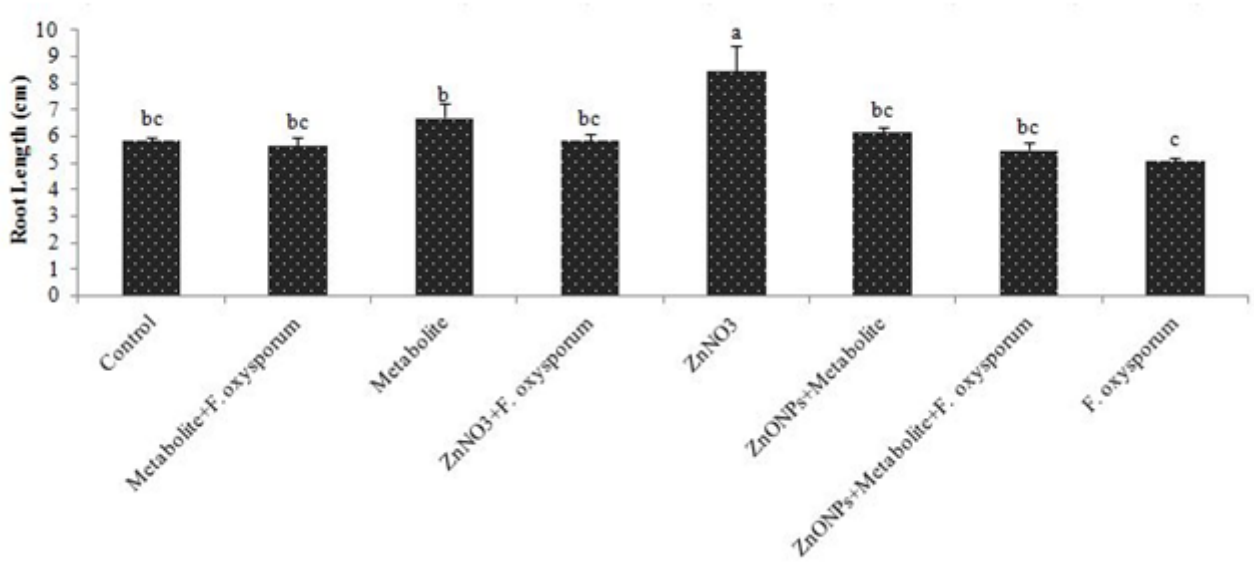

Figure 12

Improve of root length in treatments containing metabolite of *T. harzianum*, $ZnNO_3$ and ZnONPs.

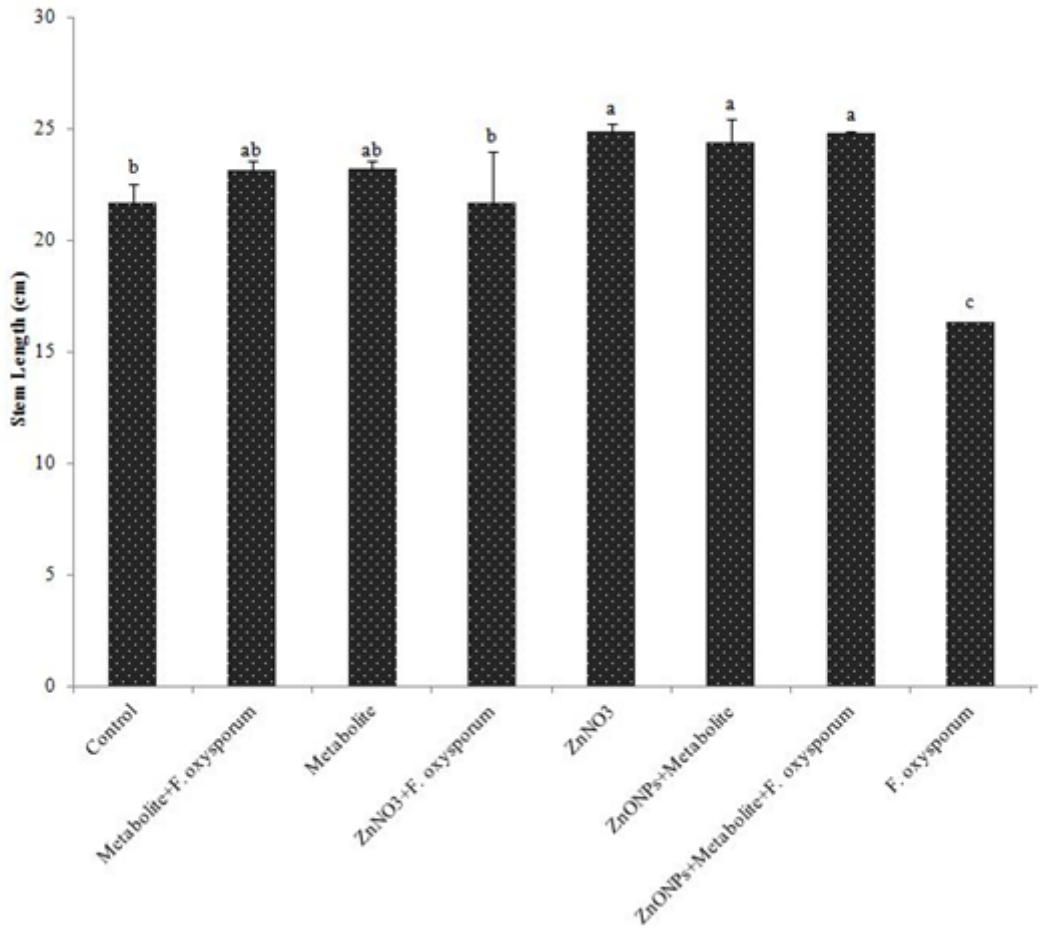

Figure 13

Improve of stem length in treatments containing metabolite of *T. harzianum*, $ZnNO_3$ and ZnONPs.

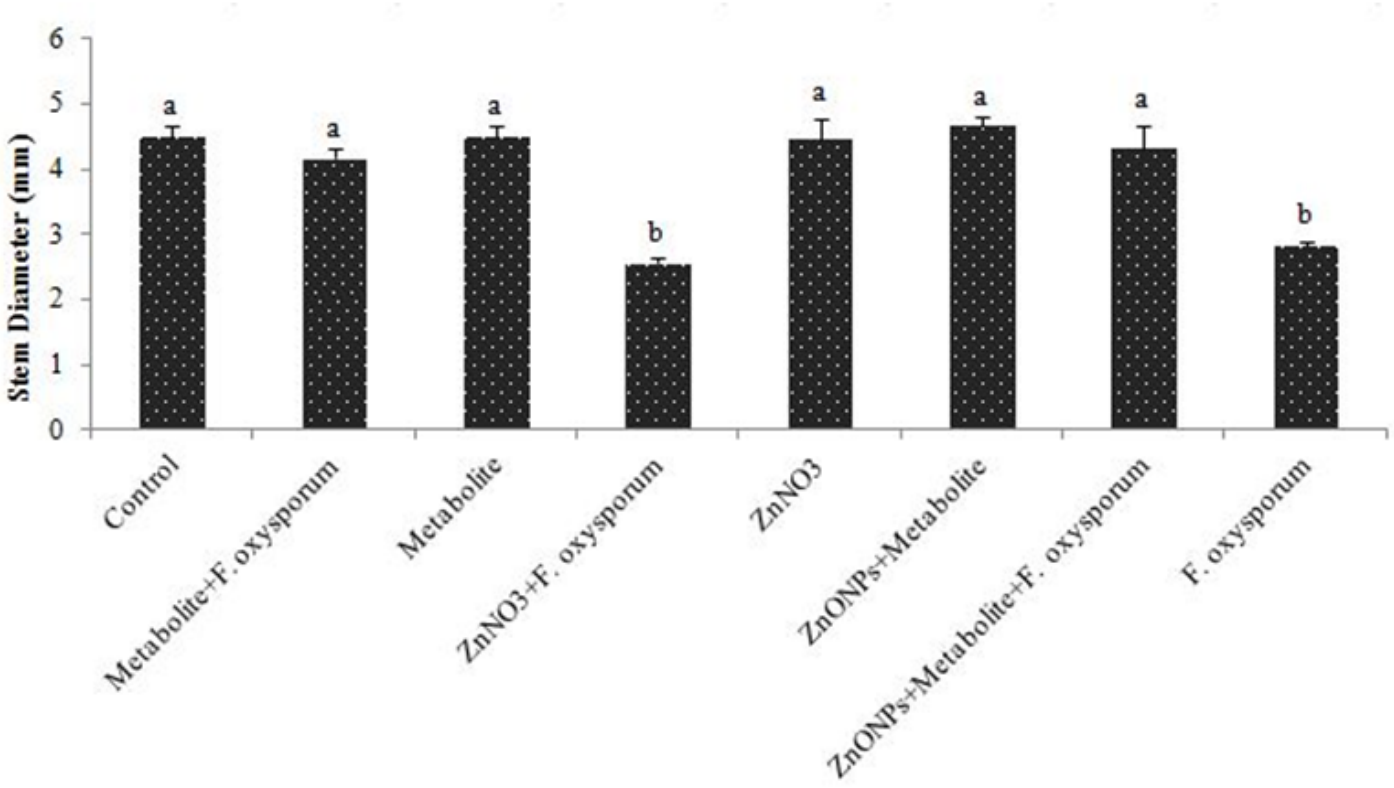

Figure 14

Improve of stem diameter in treatments containing metabolite of *T. harzianum*, $ZnNO_3$ and ZnONPs.

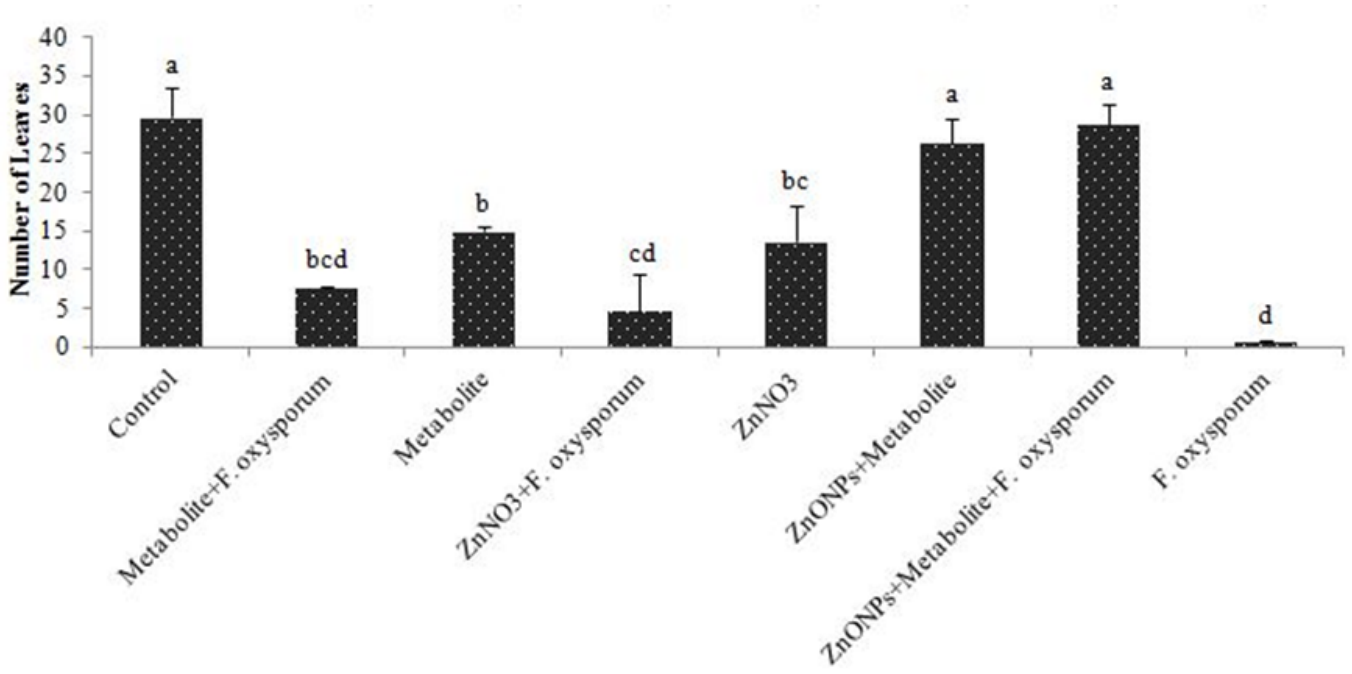

Figure 15

Improve in the number of leaves in the *F. oxysporum*+ZnONPs+metabolitetreatment